Hydrogen Chemistry and Transport Coefficients for Simulation of the DC-RF thruster TIHTUS with the Loosely Coupled Navier-Stokes Code SINA

IEPC-2011-084

U. Bauder[*]

Institut für Raumfahrtsysteme, Universität Stuttgart, 70569 Stuttgart, Germany

and

M. Auweter-Kurtz[†]

German Aerospace Academy ASA, 71304 Böblingen, Germany

For the numerical simulation of electric propulsion systems, accurate models are required to predict the chemical composition and the transport coefficients for a partially ionized plasma in chemical and thermal non-equilibrium. For hydrogen, the two chemistry models of Scott (7 species) and of Rhodes and Keefer (4 species) are adapted for the loosely coupled Navier-Stokes Code SINA. This adaption process includes the neglection of the ion H_3^+ and of excited species. For the computation of the transport coefficients, the collision integrals for the models of Chapman and Cowling and of Yos are fitted and the results of the different models are compared to values from literature for chemical equilibrium. The combination of the model of Scott for the composition and the transport coefficients computed by the model of Chapman and Cowling is in good agreement with the data in literature and therefore recommended for future simulations of the hybrid DC-RF thruster TIHTUS.

Nomenclature

$A^*,...,I^*$	= quotients of collision integrals
c	= concentration
c_v	= specific heat capacity
D_{ij}	= binary diffusion coefficient
$D_{i,m}$	= effective diffusion coefficient
$\tilde{G}^0$	= free standard enthalpy
$\tilde{H}^0$	= standard enthalpy
$\vec{j_i}$	= diffusion flux of species i
K_c	= equilibrium constant (based on concentration)
K_p	= equilibrium constant (based on pressure)
k_f	= forward reaction rate coefficient
k_b	= backward reaction rate coefficient
M	= molar mass

[*]Scientist, Modeling and Simulation of Plasma Flows, bauder@irs.uni-stuttgart.de
[†]Professor, Head of German Aerospace Academy, m.auweter-kurtz@german-asa.de

$\overline{M}$	=	mean molar mass
m	=	mass
n	=	number density
p	=	pressure
p_i	=	partial pressure of species i
R	=	specific gas constant
$\tilde{S}^0$	=	standard entropy
T	=	temperature
T*	=	reduced temperature
$\vec{v}$	=	flow velocity
X$_i$	=	species i
Z	=	charge number
z$_s$	=	number of species
z$_r$	=	number of reactions

Constants

$\mathfrak{R}$	=	universal gas constant
h	=	Planck constant
k	=	Boltzmann constant
ϵ_0	=	vacuum permittivity

Greek symbols

$\Delta^{(l)}$	=	abbreviation for collision integrals
η	=	viscosity
Θ	=	charakteristic temperature
λ	=	thermal conductivity
λ_D	=	Debye length
μ_{ij}	=	reduced mass
ν_i	=	net stoichiometric coefficient
ν_i'	=	stoichiometric coefficient of educt i
ν_i''	=	stoichiometric coefficient of product i
ξ	=	mass fraction
σ	=	cross section
υ	=	quantum number
ψ	=	molar fraction
$\overline{\Omega}_{ij}^{(l,s)}$	=	collision integral
ω_f	=	speed of forward reaction
ω_b	=	speed of backward reaction
ω_{eff}	=	effective speed of reaction
ω_i	=	production rate of specie i

Indices

eq	=	equilibrium
e	=	electron
mix	=	mixture
trans	=	translational
rot	=	rotational
vib	=	vibrational
int	=	internal

I.   Introduction

The effective exit velocity of an electric propulsion system c_e is proportional to $\sqrt{T_0/M_{eff}}$. To increase the velocity, hydrogen is used as propellant for many electric propulsion systems, because of its low molecular mass. It is also used for the hybrid DC-RF plasma thruster TIHTUS (Thermal-Inductively Heated Thruster of the University of Stuttgart).[1] The pressure in such a device is low, the temperatures and velocities are high. The high temperatures of the gas lead to dissociation and ionisation. Due to the low pressure, the collision frequencies are low and as a result the relaxation times are also high. In combination with the high gas velocity, this causes chemical and thermal non-equilibrium within the physical domain of the thruster. Hence, in order to accurately simulate the plasma flow in an electric propulsion system, the physical model of the simulation must account for a non-equilibrium composition and temperatures. This includes the model for the chemical composition as well as the model for the transport coefficients and the energy balances for the electron temperature and the internal degrees of freedom.
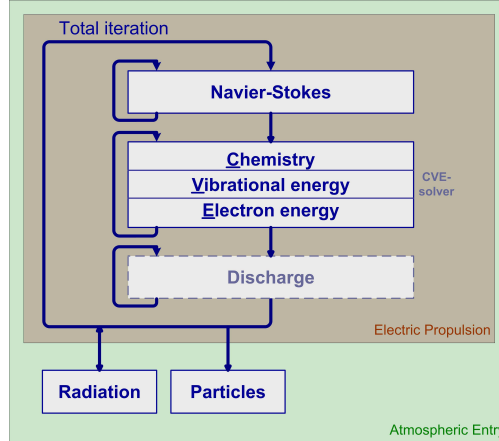

Figure 1.   iteration scheme of SINA with the different solvers[2]

For the numerical simulation of TIHTUS the loosely coupled Navier-Stokes code SINA[2] will be used. The iteration scheme of SINA is shown in Fig. 1. The main part of SINA consists of three solvers:

- The first solver within this loop computes the flow field assuming frozen flow. This so called Navier-Stokes solver accounts for mass, momentum and energy conservation according to the Navier-Stokes equations.

- The second solver contains the equations that are necessary to describe the real gas: the chemical reactions, the equations for vibrational energy of the molecules and an electron energy balance equation. Whithin this so called CVE-solver, the conserved quantities as a solution from the first solver are kept constant.

- The third solver, which is the last within one total iteration loop, solves the discharge equation of an electric arc and delivers the source terms for the energy conservation equation and the momentum conservation equation of the first solver for the next total iteration loop. This solver is not yet adapted to the new CVE-solver and therefore not available at present.

The total iteration loop is repeated until convergence is reached in all solvers and the result is the solution of the steady-state problem. Additionally, trajectories of dust particles within the flow as well as radiation transport can be accounted for using the particle solver or the external programs HERTA and PARADE for the simulation of radiation transport phenomena. Since the coupling to the flow field solution is not as strong as for the chemistry and the electric discharge, these solvers are coupled to the iteration scheme outside of the total iteration loop and are run only once per several total iterations for a numerical solution of a given problem.

In order to numerically simulate the hybrid DC-RF thruster TIHTUS, SINA has to be improved.[2] The structure of the CVE-solver and the routines for the computation have already been changed.[3] The necessary

datasets for the computation of the chemical composition of the non-equilibrium hydrogen plasma and the dataset for the computation of the according transport properties for the flow calculations are presented in this paper. In the first section, two chemistry models are adapted for the use of SINA. Then, two models for the transport properties are described, both using collision integrals. With these models, SINA computed the equilibrium composition of the hydrogen plasma for different temperatures and pressures. In the last section, these results are compared to existing data for chemical equilibrium.

II. Chemical composition

The relatively high temperatures in the discharge region and thereafter lead to dissoziation and ionization in the gas. As stated earlier, the low pressure causes high relaxation times and the high velocity causes short characteristic times. This leads to chemical non-equilibrium, at least in parts of the computational domain. Therefore the species balance equation

$$\frac{d}{dt}c_i = -\nabla c_i \vec{v} + \omega_i + \vec{j_i} \tag{1}$$

contains the convection $-\nabla c_i \vec{v}$, the chemical production ω_i and diffusion $\vec{j_i}$. The chemical production term is the result of a chemical reaction system, that has to be as detailed as necessary. An arbitrary chemical reaction equation of such a model can be written as

$$\sum_{i=1}^{z_s} \nu_i' X_i \underset{k_b}{\overset{k_f}{\rightleftharpoons}} \sum_{j=1}^{z_s} \nu_j'' X_j, \tag{2}$$

where ν_i' and ν_j'' are the stoichiometric coefficients of the educts X_i and products X_j, respectively. The reaction rate coefficients k_f and k_b describe the speed of the forward and backward reaction. The speed of the forward reaction

$$\omega_f = k_f \prod_{i=1}^{z_s} c_{X_i}^{\nu_i'} \tag{3}$$

and backward reaction

$$\omega_b = k_b \prod_{i=1}^{z_s} c_{X_i}^{\nu_i''} \tag{4}$$

depend on the concentrations c_i of the reacting species. The production rate of the species i for the species balance equation (Eq. 1) then is

$$\omega_i = \sum_{r=1}^{z_r} \nu_{i,r} \omega_{eff,r} \ , \tag{5}$$

with the net stoichiometric coefficient $\nu_{i,r} = \nu_{i,r}'' - \nu_{i,r}'$ and the effective speed of reaction $\omega_{eff,r} = \omega_{f,r} - \omega_{b,r}$. The reaction scheme provides the stoichiometric coefficients. Additionally, the forward reaction rates are given in the form of the Arrhenius function

$$k = C \cdot T^s e^{\frac{-T_a}{T}}. \tag{6}$$

Here, $T_a = E_a/\Re$ is the temperature corresponding to the activation energy E_a, C is the Arrhenius constant and S the temperature coefficient that describes the temperature dependancy of the preexponential factor. In a multitemperature model, T may differ from the translational temperature of the heavy species. The simple T-Tvib model of Park[4] is used in SINA for multitemperature calculations.

The backward reaction coefficient is computed from the equilibrium constant. In chemical equilibrium, ω_f and ω_b are identical and one obtains the equilibrium constant

$$K_c = \frac{k_f}{k_b} = \left(\frac{\prod_{i=1}^{z_s} c_{X_i}^{\nu_i''}}{\prod_{j=1}^{z_s} c_{X_j}^{\nu_j'}} \right)_{eq} = \left(\prod_{i=1}^{z_s} c_{X_i}^{\nu_i} \right)_{eq} \tag{7}$$

and from this the rate coefficient for the backward reaction

$$k_b = \frac{k_f}{K_c} \ . \tag{8}$$

The equilibrium constant can be obtained from minimizing Gibbs free energy for each reaction when the standard enthalpy $\tilde{H}^0$ and standard entropy $\tilde{S}^0$ of the species are known. This procedure leads to a physical consistent and accurate equilibrium constant. Usually, it is much more accurate than the measurement of both the forward and backward reaction rates and ensures an accurate prediction of the composition for the equilibrium case. The temperature dependant equilibrium constant is fitted with the polynomial function

$$
\begin{aligned}
K_c(T) = \exp \Bigg(& P_{K,1} + P_{K,2} \ln(\frac{T}{1000}) + P_{K,3}(\frac{T}{1000})^{-1} + P_{K,4}(\frac{T}{1000})^{-2} \\
& + P_{K,5}(\frac{T}{1000})^{-3} + P_{K,6}\frac{T}{1000} + P_{K,7}(\frac{T}{1000})^2 + P_{K,8}(\frac{T}{1000})^3 + P_{K,9}(\frac{T}{1000})^4 \Bigg)
\end{aligned}
\tag{9}
$$

and given to SINA in the same input file as the reaction scheme and the data for the rate coefficient for the forward reaction.

SINA has some limitations regarding the physical phenomena connected to the chemical reaction systems.

- The species are assumed to be in their ground state. Electronically excited states are neglected.

- The vibrational energy model assumes two-atomic molecules. Molecules with more than two atoms require a code improvement.

- Radiation emitted by chemical reactions can not be traced correctly but will increase the translational energy and hence the translational temperature.

- Each specified reaction always takes place both in forward and backward direction.

A. Adaption of the model of Scott

For microwave plasmas, Scott developed a hydrogen chemistry model that is given in Table A and consist of the seven species H_2, H, H_3^+, H_2^+, H^+, H^- und electrons.[5] The ion H_3^+ is a three-atomic molecule and hence the simple assumption of a truncated harmonic oscillator model for the vibrational energy is not applicable without modifications. There are, in principle, two ways to deal with this issue. The first is to neglect this ion in the reaction scheme since the mole fraction of H_3^+ is always below 10^{-12} in an equilibrium composition below $1\,\mathrm{bar}$.[6] The second possibility is to improve the vibrational energy model in order to achieve a physically consistent description of the vibrational energy. This is the long-term goal for SINA. In the context of this paper, H_3^+ is neglected in SINA.

The reaction system of Scott consists of 27 reactions. Note that it consists of forward reactions only. Backward reactions are neglected, if not given explicitly as a seperate forward reaction. For the usage in SINA, the scheme in Table A has to be adopted:

1. Reactions with $H_2(v)$ also contain H_2 molecules in the ground state. They remain in the reaction scheme.

2. Reactions 5, 7, 9, 20 and 22 contain excited states and are neglected.

3. Reactions 4, 5, 6, 16, 24 and 27 contain H_3^+ and are neglected.

4. Reaction 12 emits radiation and is neglected.

5. Within the remaining 16 reactions, the reactions 10, 13, 14 and 15 are backward reactions of 2, 17, 18 und 21. These are already represented by the corresponding forward reactions and their backward reactions in SINA.

With these changes, 12 reactions for the remaining 6 species remain, plus their backward reactions. The system is shown in Table A with the parameters for the Arrhenius equation for the forward reaction rate coefficients. The equilibrium constants for the backward rate coefficients are computed by minimizing Gibbs free energy, as stated earlier. The data for the standard enthalpy of formation and standard entropy of

1	$e^- + H_2(v) \longrightarrow e^- + H_2^+ + e^-$	15	$H_2^+ + H \longrightarrow H^+ + H_2$	
2	$e^- + H \longrightarrow e^- + H^+ + e^-$	16	$H_2^+ + H_2 \longrightarrow H_3^+ + H$	
3	$e^- + H_2(v) \longrightarrow e^- \ H_2^* \longrightarrow e^- + H + H$	17	$H_2 + H_2 \longrightarrow H + H + H_2$	
4	$e^- + H_3^+ \longrightarrow H + H + H$	18	$H_2 + H \longrightarrow H + H + H$	
5	$e^- + H_3^+ \longrightarrow H_2(v>5) + H(n{=}2)$	19	$H + H^- \longrightarrow e^- + H + H$	
6	$e^- + H_3^+ \longrightarrow e^- + H^+ + H + H$	20	$H + H^- \longrightarrow e^- + H_2(v)$	
7	$e^- + H_2(v) \longrightarrow H + H^-(v \geqq 4)$	21	$H^+ + H_2 \longrightarrow H + H_2^+$	
8	$e^- + H_2^+ \longrightarrow e^- + H^+ + H$	22	$H^+ + H^- \longrightarrow H(n{=}3) + H(1s)$	
9	$e^- + H_2^+ \longrightarrow H + H(n)$	23	$e^- + e^- + H_2^+ \longrightarrow e^- + H + H$	
10	$e^- + e^- + H^+ \longrightarrow e^- + H$	24	$e^- + e^- + H_3^+ \longrightarrow e^- + H + H_2$	
11	$e^- + H^- \longrightarrow e^- + e^- + H$	25	$H^+ + H_2 + H_2 \longrightarrow H_3^+ + H_2$	
12	$e^- + H^+ \longrightarrow h\upsilon + H$	26	$H^- + H_2^+ \longrightarrow H_2 + H$	
13	$H + H + H_2 \longrightarrow H_2 + H_2$	27	$H^- + H_3^+ \longrightarrow H_2 + H_2$	
14	$H + H + H \longrightarrow H_2 + H$			

<div align="center">Table 1. Original reaction scheme of Scott [5]</div>

formation are available in tables [7] and sometimes as polynoms .[8] They are fitted over seperate temperature ranges to improve the overall accuracy, if necessary. The species data is taken from NIST .[8]

Above or below a temperature limit, the rate coefficient and equilibrium constant computed with the value of the temperature limit are used, to avoid jumps.
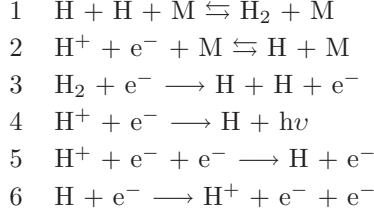
	Reaction	C	s	T_a
1	$e^- + H_2 \leftrightarrows e^- + H_2^+ + e^-$	1,18E+013	0	191500
2	$e^- + H \leftrightarrows e^- + H^+ + e^-$	1,08E+013	0	178210
3	$e^- + H_2 \leftrightarrows e^- + H + H$	1,20E+013	0	113500
4	$e^- + H_2^+ \leftrightarrows e^- + H^+ + H$	1,46E+014	0	37460
5	$e^- + H^- \leftrightarrows e^- + e^- + H$	1,34E+010	0,9	22700
6	$H_2 + H_2 \leftrightarrows H + H + H_2$	8,61E+014	-0,7	52530
7	$H_2 + H \leftrightarrows H + H + H$	2,70E+013	-0,1	52530
8	$H + H^- \leftrightarrows e^- + H + H$	4,50E+005	1,5	698
9	$H + H^- \leftrightarrows e^- + H_2$	1,43E+012	-0,15	815
10	$H^+ + H_2 \leftrightarrows H + H_2^+$	1,90E+011	0	21902
11	$e^- + e^- + H_2^+ \leftrightarrows e^- + H + H$	3,17E+015	-4,5	0
12	$H^- + H_2^+ \leftrightarrows H_2 + H$	2,08E+015	-0,5	0

<div align="center">Table 2. Modified reaction scheme of Scott</div>

B.   The model of Rhodes and Keefer

Another model for hydrogen was developed by Rhodes and Keefer for the simulation of plasma flows in thermal arc-jets .[9] The 6 reactions of this model are given in Table 3. There are no excited atoms or molecules and no specific temperature limits per reaction in this scheme. In thermal non-equilibrium, translational temperature of the heavy particles or electrons is used.

The scheme is based on the reaction rate coefficients of McCay ,[10] except for reaction 5. The electron impact ionization is a combination of two reactions: first, the hydrogen atom is excited by a first electron impact and then ionized by another electron impact. Since the second reaction is very fast, both reactions can be treated as one reaction to avoid the occurance of excited atoms in the reaction scheme. The rate coefficient for this artificial reaction was computed by Keefer .[11, 12]

Table 3. reaction scheme of Rhodes and Keefer

1	$H + H + M \leftrightarrows H_2 + M$
2	$H^+ + e^- + M \leftrightarrows H + M$
3	$H_2 + e^- \longrightarrow H + H + e^-$
4	$H^+ + e^- \longrightarrow H + h\upsilon$
5	$H^+ + e^- + e^- \longrightarrow H + e^-$
6	$H + e^- \longrightarrow H^+ + e^- + e^-$

The corresponding backward reaction is given as a seperate forward reaction (reaction 6). The artificial rate coefficient for forward reaction 5 causes an artificial equilibrium constant. For the adaption to SINA, the equilibrium constant for this reaction is computed using $K_c(T) = k_f(T)/k_b(T)$ instead of the procedure described earlier. Note that this procedure represents the 'artificial' rates of the original reaction scheme and therefore may lead to an inconsistent equilibrium composition.

For reactions 3 and 4 the equilibrium constant is computed with $K_c(T) = k_f(T)/k_b(T)$ using constant $k_b = 10^{-30}$ to eliminate the backward reaction. The emitted radiation in reaction 4 is neglected and the corresponding energy is added to the translational energy. The reason for not neglecting these reactions is the already low number of reactions in the original scheme that should not be further reduced.

The resulting reaction scheme is shown in Table B including the parameters for the forward reaction rates. Note that the reaction scheme of Rhodes and Keefer is therefore implemented in SINA without changes in the scheme itself, but only in its representation.

	Reaction	C	s	T_a
1	$H + H + M \leftrightarrows H_2 + M$	6,40E+017	-1	0
2	$H^+ + e^- + M \leftrightarrows H + M$	5,26E+026	-2,5	0
3	$H_2 + e^- \longrightarrow H + H + e^-$	1,91E+011	1	24,42
4	$H^+ + e^- \longrightarrow H$	3,77E+013	-0,58	0
5	$H + e^- \leftrightarrows H^+ + e^- + e^-$	1,81E+014	0	29436,63

Table 4. Adopted reaction scheme of Rhodes and Keefer

III. Transport coefficients

The implemented models for the computation of the transport coefficients in SINA are identical to the models available in the fully implicit, fully coupled non-equilibrium Navier Stokes Code URANUS [13,14] that is also developed at the IRS. The basic principle of both implemented models is the computation of the transport coefficients based on collision integrals. The simple model of Yos [15] is widely used.[13,16,17] The second and more accurate model is based on the first approximation of the theory of Chapman and Cowling. Both use polynomial fits for the collision integrals of the colliding pairs that are read from an input file. The models are described in detail in the literature.[13] The reduced collision integrals

$$\Omega_{ij}^{(l,s)}(T_i, T_j) = \frac{8\pi(l+1)}{(s+1)! \, [2l + 1 - (-1)^l]} \int\limits_0^\infty \int\limits_0^\infty e^{-\gamma^2} \gamma^{2s+3}(1 - \cos^l \chi(b,g)) b \, db \, d\gamma \tag{10}$$

are derived from the potential of the interaction of two colliding particles,[13,18] with the angle of deflection $\chi(b,g)$ and the relative velocity g according to the definition of Hirschfelder et al.[18] For thermal non-equilibrium of the species i and j, the reduced relative velocity γ_{ij} is

$$\gamma_{ij} = \sqrt{\frac{\mu_{ij} g_{ij}^2}{2kT_{ij}}} \tag{11}$$

with the reduced mass

$$\mu_{ij} = \frac{m_i m_j}{m_i + m_j} \tag{12}$$

and

$$T_{ij} = \frac{m_i T_j + m_j T_i}{m_i + m_j} \ . \tag{13}$$

The collision of two charged particles is dominated by the Coulomb forces.[19] Hence, the collision integrals

$$\overline{\Omega}_{ij}^{(l,s)}(T_i, T_j) = \pi(\lambda_D/T_{ij}^*)^2 \Omega_{ij}^{(l,s)*}(T_{ij}^*) \tag{14}$$

depend on the charges of the colliding particles only. Here, $\Omega_{ij}^{(l,s)*}$ are the dimensionless collision integrals of Mason et. al,[19]

$$\lambda_D = \sqrt{\frac{\epsilon_0 k}{e^2} \left(\frac{n_e}{T_e} + \sum_{i=Ion} \frac{Z_i^2}{T_i} n_i \right)^{-1}} \tag{15}$$

is the Debye length and the non-dimensional temperature is

$$T_{ij}^* = \lambda_D (e^2/4\pi\epsilon_0 k T_{ij})^{-1} \ . \tag{16}$$

For the following equations, the two abbreviations

$$\Delta_{ij}^{(1)} = \frac{8}{3} \sqrt{2\mu_{ij}/\pi k T_{ij}} \, \overline{\Omega}_{ij}^{(1,1)} \tag{17}$$

and

$$\Delta_{ij}^{(2)} = \frac{16}{5} \sqrt{2\mu_{ij}/\pi k T_{ij}} \, \overline{\Omega}_{ij}^{(2,2)} \tag{18}$$

and the two quotients

$$A_{ij}^* = \frac{\overline{\Omega}_{ij}^{(2,2)}}{\overline{\Omega}_{ij}^{(1,1)}} \tag{19}$$

and

$$B_{ij}^* = \frac{5\overline{\Omega}_{ij}^{(1,2)} - 4\overline{\Omega}_{ij}^{(1,3)}}{\overline{\Omega}_{ij}^{(1,1)}} \tag{20}$$

are used.

A. Diffusion

At constant pressure and temperature, a gradient in the concentration $\frac{dn_1}{y} = -\frac{dn_2}{dy}$ in a mixture of two gases with the number densities n_1 and n_2 causes two diffusion fluxes with the flux densities

$$\vec{j_1} = -\vec{j_2} = -D_{12}\frac{dn_1}{dy} \ , \tag{21}$$

where the proprotionality factor D_{12} is the binary diffusion coefficient of gas 1 in gas 2. Assuming that only one component diffuses, the diffusion flux is[20]

$$\vec{j_i} = -\rho D_{i,eff} \nabla \psi_i \ , \tag{22}$$

where $D_{i,m}$ is the effective diffusion coefficient

$$D_{i,m} = \frac{M_i(1 - \xi_i)}{\overline{M} \sum_{j=1\ j \neq i}^{z_s} \psi_j / D_{ij}} \qquad (23)$$

with the binary diffusion coefficient

$$D_{ij} = D_{ji} = \frac{3}{16} \frac{\sqrt{2\pi k^3 T^3}}{p \overline{\Omega}_{ij}^{(1,1)} \sqrt{\mu_{ij}}} \; . \qquad (24)$$

Ambipolar diffusion

The difference in diffusion velocity of electrons and ions generates an ambipolar electric field, that can be regarded as an external force working on the diffusion fluxes in such a way that it reduces the diffusion speed of the electrons and increases the speed of the ions. This force is not included in the equations above and the resulting diffusion coefficient for ions is too low. According to an estimation of Lee,[21] the effective ambipolar diffusion coefficient is twice the diffusion coefficient for ions: $D_{ion,m}^a \approx 2D_{ion,m}$, such that:

$$D_{i,eff} = \begin{cases} D_{i,m} \text{ for neutral species} \\ 2D_{i,m} \text{ for ions} \end{cases} \qquad (25)$$

B. Viscosity

The viscosity η of a mixture of gases is [18]

$$\eta_{mix} = \sum_{j=1}^{z_s} \psi_j \left(\frac{nkT_j}{2} b_{j0} \right) \qquad (26)$$

where n is the number density and b_{j0} are the so-called Sonine coefficients with

$$\psi_i = \sum_{j=1}^{z_s} H_{ij} \left(\frac{nkT_j}{2} b_{j0} \right) , \qquad (27)$$

$$H_{ii} = \frac{\psi_i^2}{m_i} \Delta_{ii}^{(2)} + \sum_{j=1\ j \neq i}^{z_s} \frac{\psi_i \psi_j}{m_i + m_j} \Delta_{ij}^2 \left[\frac{5}{3A_{ij}^*} + \frac{m_j}{m_i} \right] \qquad (28)$$

and

$$H_{ij} = \frac{\psi_i \psi_j}{m_i + m_j} \Delta_{ij}^{(2)} \left[1 - \frac{5}{3A_{ij}^*} \right], \qquad i \neq j \; . \qquad (29)$$

C. Heat conduction

The heat flux $\dot{\vec{q}}$ in a gas with a temperature gradient $\frac{\delta T}{\delta x}$ is

$$\dot{\vec{q}} = -\lambda \frac{\delta T}{\delta x} \qquad (30)$$

with the thermal conductivity λ. The computation of the thermal conductivity is different for the model of Chapman and Cowling (CC) and the model of Yos. The CC model considers the heat conductivity of the internal degrees of freedom for rotation and vibration in addition to the translational thermal conductivity.[13]

Heat conductivity of the heavy particles

According to Brokaw,[22] the translational thermal conductivity of a gas mixture can be approximated by

$$\lambda_{mix,trans} \approx \frac{15k}{4} \sum_{i=1}^{z_s} \frac{\psi_i}{\sum_{j=1}^{z_s} \alpha_{ij} \psi_j \Delta_{ij}^{(2)}} \, , \tag{31}$$

with

$$\alpha_{ij} = \frac{\left(\frac{m_i}{m_j} - 1\right)\left(\left[\frac{3}{2}\frac{B_{ij}^*}{A_{ij}^*} - \frac{25}{8A_{ij}^*} + 1\right] + \left[\frac{15}{4A_{ij}^*} - 1\right]\frac{m_i}{m_j}\right)}{\left(1 + \frac{m_i}{m_j}\right)^2} \, . \tag{32}$$

Heat conductivity of electrons

The thermal conductivity of electrons is computed by [23]

$$\lambda_{mix,e} = \frac{\psi_e^2}{L_{ee}^{11} + \frac{(L_{ee}^{12})^2}{L_{ee}^{22}}} \tag{33}$$

with the abbreviations

$$L_{ee}^{11} = \frac{\psi_e}{k}\left\{\frac{4}{15}\psi_e\Delta_{ee}^{(1)} + \sum_{k=1\,k\neq e}^{z_s} \frac{\psi_k\Delta_{ek}^{(1)}}{(m_e+m_k)^2}\left[\frac{16}{25}A_{ek}^* m_e m_k + \left(1 - \frac{12}{25}B_{ek}^*\right)m_k^2 + \frac{6}{5}m_e^2\right]\right\}, \tag{34}$$

$$
\begin{aligned}
L_{ee}^{12} \approx \frac{\psi_e}{k}\Bigg\{ &\psi_e\Delta_{ee}^{(2)}\left(\frac{7}{15} - \frac{8}{15}E_{ee}^*\right) \\
&+ \sum_{k=1\,k\neq e}^{z_s} \psi_k\Delta_{ek}^{(1)}\left[\frac{7}{4} - \frac{57}{25}B_{ek}^* + \frac{51}{10}C_{ek}^* - \frac{24}{5}G_{ek}^*\right]\Bigg\},
\end{aligned}
\tag{35}
$$

and

$$
\begin{aligned}
L_{ee}^{22} \approx \frac{\psi_e}{k}\Bigg\{ &\psi_e\Delta_{ee}^{(2)}\left(\frac{77}{60} - \frac{28}{15}E_{ee}^* + \frac{4}{3}H_{ee}^*\right) \\
&+ \sum_{k=1\,k\neq e}^{z_s} \psi_k\Delta_{ek}^{(1)}\left[\frac{49}{16} - \frac{399}{50}B_{ek}^* + \frac{126}{5}C_{ek}^* - \frac{168}{5}G_{ek}^* + \frac{72}{5}I_{ek}^*\right]\Bigg\}
\end{aligned}
\tag{36}
$$

and the quotients

$$C_{ij}^* = \frac{\overline{\Omega}_{ij}^{(1,2)}}{\overline{\Omega}_{ij}^{(1,1)}}, \quad G_{ij}^* = \frac{\overline{\Omega}_{ij}^{(1,4)}}{\overline{\Omega}_{ij}^{(1,1)}}, \quad I_{ij}^* = \frac{\overline{\Omega}_{ij}^{(1,5)}}{\overline{\Omega}_{ij}^{(1,1)}}$$

and

$$E_{ij}^* = \frac{\overline{\Omega}_{ij}^{(2,3)}}{\overline{\Omega}_{ij}^{(2,2)}}, \quad H_{ij}^* = \frac{\overline{\Omega}_{ij}^{(2,4)}}{\overline{\Omega}_{ij}^{(1,2)}} \, . \tag{37}$$

Thermal conductivity of internal degrees of freedom

The collision integrals do not contain any information on the internal strucure of the colliding species. Therefore, the thermal conductivity of internal degrees of freedom is computed by the formula of Brokaw [21]

$$\lambda_{mix,int} = k \sum_i \frac{(c_{v,int,i}/R_i)\frac{5}{6A_{ii}^*}\psi_i}{\sum_j \Delta_{ij}^{(1)}\psi_j} \, ,$$ (38)

that considers the transport of internal energy by diffusion. The specific heat capacities are as follows:

- For the rotational energy a rigid rotator is used, truncated at the dissociation energy:

$$c_{v,rot,i} = R_i \left\{ 1 - \left[\frac{\frac{\Theta_{D,i}}{2T_{rot,i}}}{\sinh\left(\frac{\Theta_{D,i}}{2T_{rot,i}}\right)} \right]^2 \right\}$$ (39)

- For the vibrational energy the model of the truncated harmonic oscillator is used:

$$c_{v,vib,i} = R_i \left\{ \left[\frac{\frac{\Theta_{vib,i}}{2T_{vib,i}}}{\sinh\left(\frac{\Theta_{vib,i}}{2T_{vib,i}}\right)} \right]^2 - \left[\frac{\frac{\Theta_{D,i}}{2T_{vib,i}}}{\sinh\left(\frac{\Theta_{D,i}}{2T_{vib,i}}\right)} \right]^2 \right\}$$ (40)

As stated earlier, only the collision integrals are needed for the computation of the transport coefficients. The collision integrals are provided to SINA in polynomial form. For each possible pair of collision, the diffusion collision integral $\overline{\Omega}_{ij}^{(1,1)}$, viscosity collision integral $\overline{\Omega}_{ij}^{(2,2)}$ and the quotient B_{ij}^* have to be provided. For the computation of the higher order electron thermal conductivity in the model of Chapman and Cowling, the collision integrals $\overline{\Omega}_{ex}^{(l,s)}$ for all collisions with electrons for $l = 1; 2$ and $s = 1...5$ are needed additionally.

The 21 possible collisions can be separated into the following categories
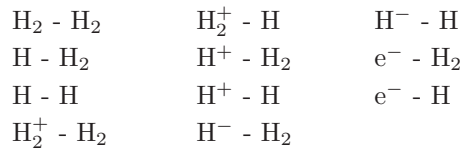
- collisions of equally charged particles

$$H_2^+ \text{ - } H_2^+ \qquad H^+ \text{ - } H^+ \qquad e^- \text{ - } H^-$$
$$H^+ \text{ - } H_2^+ \qquad H^- \text{ - } H^- \qquad e^- \text{ - } e^-$$
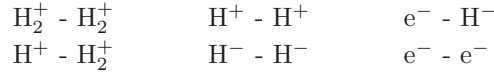
- collisions of oppositely charged particles

$$H^- \text{ - } H_2^+ \qquad e^- \text{ - } H_2^+$$
$$H^- \text{ - } H^+ \qquad e^- \text{ - } H^+$$

- collisions of two neutral particles or neutrals with ions

$$H_2 \text{ - } H_2 \qquad H_2^+ \text{ - } H \qquad H^- \text{ - } H$$
$$H \text{ - } H_2 \qquad H^+ \text{ - } H_2 \qquad e^- \text{ - } H_2$$
$$H \text{ - } H \qquad H^+ \text{ - } H \qquad e^- \text{ - } H$$
$$H_2^+ \text{ - } H_2 \qquad H^- \text{ - } H_2$$

- collisions of electrons with neutrals

$$e^- \text{ - } H_2 \qquad e^- \text{ - } H$$

- collisions of electrons with ions

$$e^- \text{ - } H^- \qquad e^- \text{ - } H_2^+$$
$$e^- \text{ - } e^- \qquad e^- \text{ - } H^+$$

For the collisions of two charged particles the collision integrals depend on the charge number of the particles only. Therefore, the polynomial coefficients can be taken from the model of air.[13] The parameters for the collisions of electrons and ions can be taken from that model as well. For most of the other collisions, the integrals can be found in literature. Where available, the collision integrals were taken from Capitelli[24] and fitted to the polynomials using MATLAB. Since Capitelli[24] has no integrals for the collisions H_2 - e and H - e as well as for collisions between neutrals and the ions H_2^+ and H^-, these are taken from Brandel.[16] Data for the collisions of the ions H_2^+ and H^- and neutrals could not be found. They were computed using the analytical method based on a modified form of the Lennard-Jones potential.[25] The computation was done in MATLAB and the results can be found in the thesis of Höptner.[26]

Accuracy of the polynomials

The polynomials for the collision integrals for the diffusion and the viscosity represent the course of the functions with good accuracy, but the polynomial for B_{ij}^* is not able to describe the function of the quotient of the collision integrals accurately. The maximum error is 30 %. This has to be adressed by a more apropriate polynomial in future versions of SINA. For the collision integrals of electron collisions it was not possible to determine the polynomial factors without a deviation of about one order of magnitude at high temperatures.
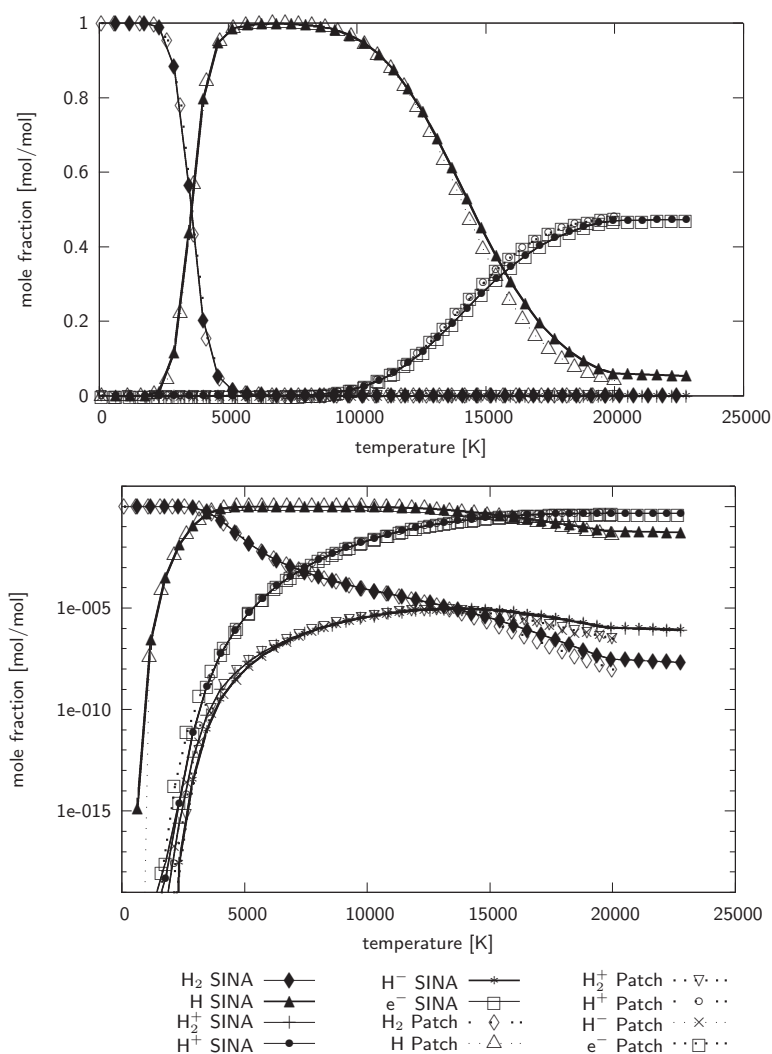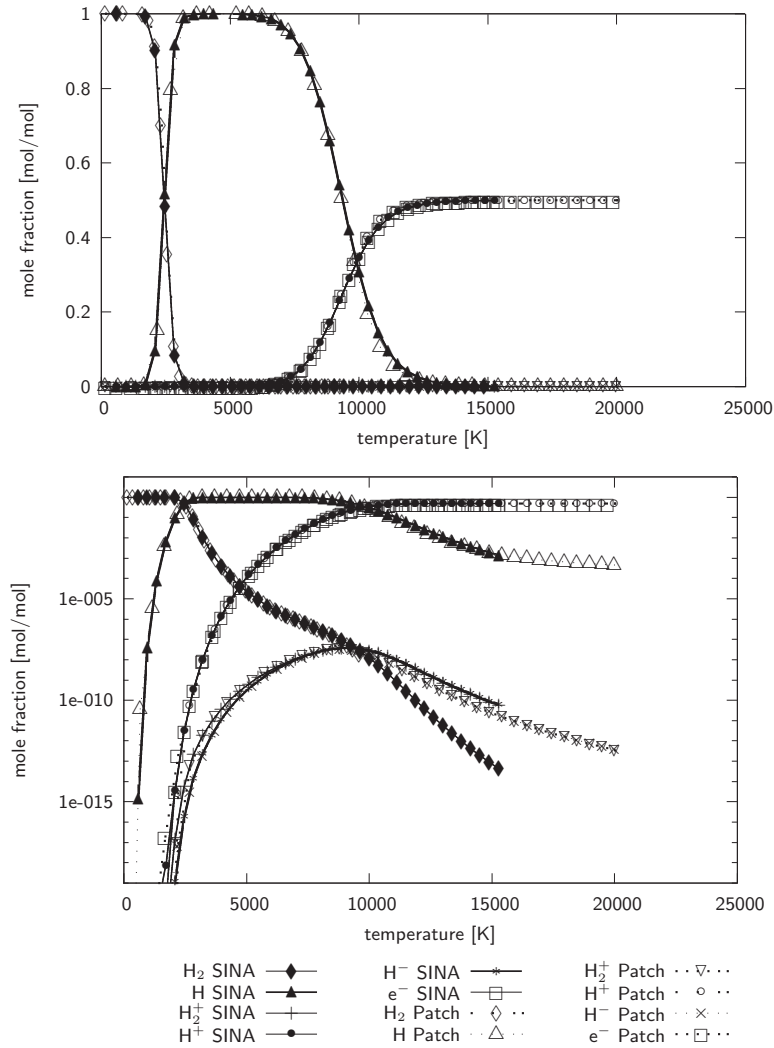

Figure 2. Equilibrium composition of hydrogen at 100000 Pa computed with the modified reaction scheme of Scott

IV.   Results and Comparison

In order to verify the implemented code and the datasets, a comparison is made to data available in literature for the chemical composition in equilibrium and the corresponding transport coefficients. The results of both chemistry models and both models for the computation of the transport coefficients are compared to each other.

A.   Chemical composition in equilibrium

The chemical composition (and the transport coefficients) in non-equilibrium is difficult to measure with the necessary accuracy. Therefore, the comparison is made in chemical equilibrium. Note that a comparison of the composition in equilibrium primarily is a validation of the equilibrium constant. It also may detect severe problems in the rate coefficients, but can not validate them. This has to be done with a comparison of more sophisticated and more complex experiments dealing with a greater number of physical aspects in non-equilibrium flows.
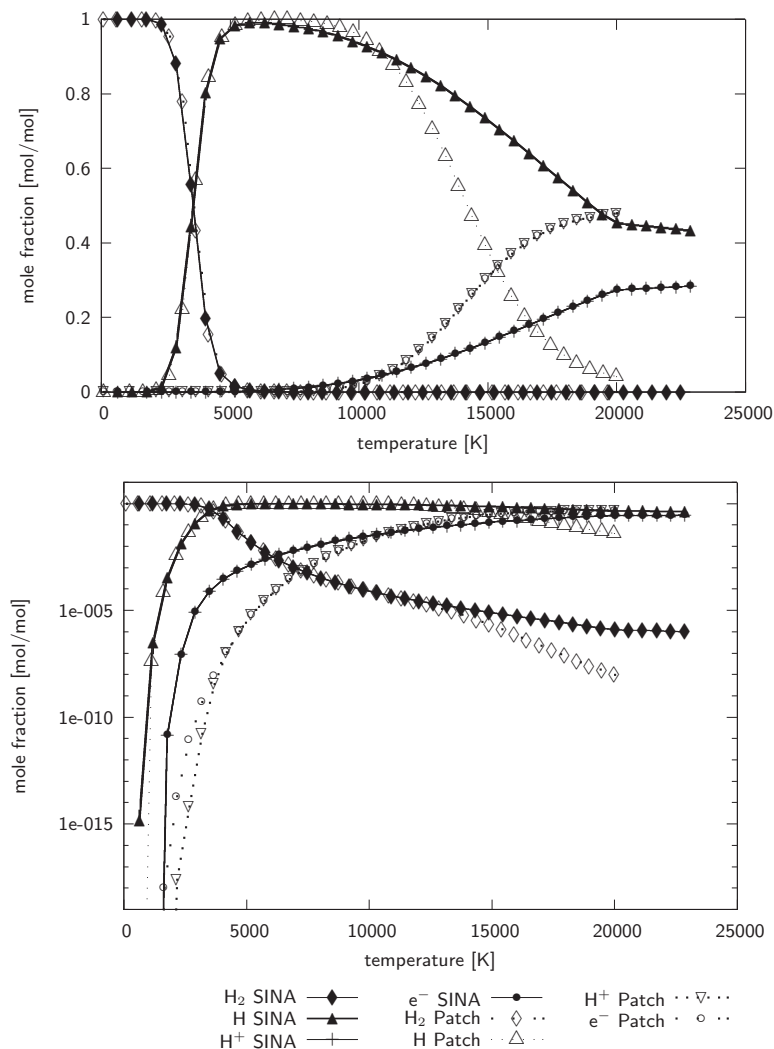

Figure 3. Equilibrium composition of hydrogen at 100 Pa computed with the modified reaction scheme of Scott

The equilibrium composition computed by SINA with both models is compared to the data of Patch [6] for $100\,\text{Pa}$ and $100000\,\text{Pa}$. For the transport coefficients, the species concentrations above 10^{-2} are significant. Hence, the upper diagrams in the following figures show the linear scaling of the mole fraction, while the lower

diagrams show a logarithmic scale to valuate the chemical composition for species with lower concentration.

The upper diagram in Fig. C shows the chemical composition computed by SINA with the modified model of Scott compared to the data of Patch for a linear scale. The overall agreement of the data is very good. Above 12000 K the concentration computed by SINA is slightly higher than the data of Patch. Accordingly, the concentration of H^+ and e^- is slightly lower. The lower plot with the logarithmic scale shows a very good agreement for the lower concentrations, too. Fig. A shows the same comparison for a pressure of 100 Pa. The overall agreement of the data is even better than for 100000 Pa as can be seen in both the linear and logarithmic plot.

Figure 4. Equilibrium composition of hydrogen at 100000 Pa computed with the reaction scheme of Rhodes & Keefer

The comparison of the results from the model of Rhodes and Keefer to the data of Patch for 100000 Pa in Fig. A shows a significantly worse concurrence. Up to 10000 K the model performs reasonably well, but above this temperature the ionization region of H is not reproduced correctly and the molar fractions of H, H^+ and e^- differ from the Patch data.

At a pressure of 100 Pa the result is slightly better. Above around 11000 K the agreement in the ionization process is better, but between 4000 K and 11000 K the discrepancy is significant. The results show that the model of Rhodes and Keefer can not reproduce the transition from the dissociated haydrogen plasma to the ionized plasma correctly. At lower pressures, this transition occurs at lower temperatures. At 100 Pa one can see a good agreement for the fully ionized plasma at very high temperatures. At 100000 Pa this region lies above the maximum temperature of 20000 K and is not visible in the diagrams. This is in accordance
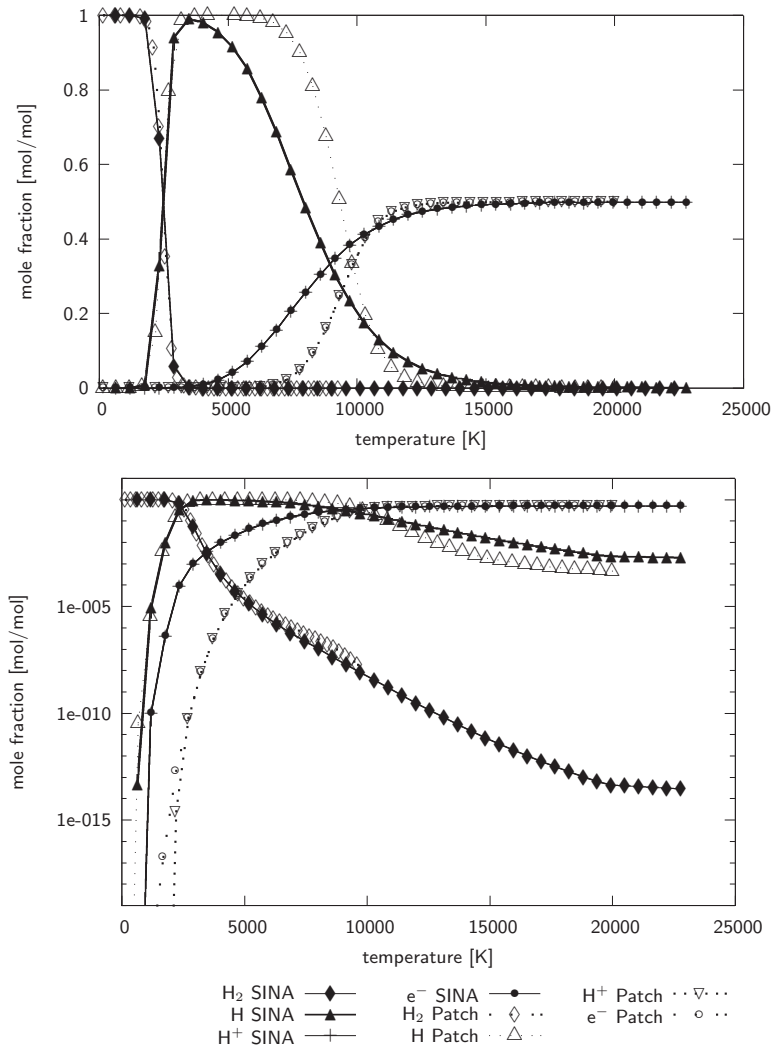
Figure 5. Equilibrium composition of hydrogen at 100 Pa computed with the reaction scheme of Rhodes & Keefer

with the results of Hermann .[27]

B. Transport coefficients for a composition in chemical equilibrium

With the results from both chemistry models for the equilibrium composition at 100000 Pa the transport coefficients are computed with both the model of Yos and the model of Chapman and Cowling. The viscosity and the frozen thermal conductivity are compared to data of Capitelli ,[28] Devoto [29] and Yos.[20]

The viscosity and the frozen thermal conductivity from the model of Yos are to be compared to the data from Yos,[20] while the results from the model of Chapman and Cowling have to be compared to the data of Capitelli [28] and Devoto .[29] In Fig. B, the viscosity computed using the model of Yos for the composition computed with the model of Scott is in reasonable agreement with the data of Yos. At high temperatures, the difference is still below 30 %.

The comparison is much better for the model of Chapman and Cowling, as can be seen in Fig. B. Note that the results have to be compared to the data of Capitelli [28] and Devoto [29] in this case. The same behaviour is observed for the frozen thermal conductivity for the model of Yos in Fig. B and for the model of Chapman and Cowling in Fig. B.

The same comparisons are made based on the chemical composition computed with the model of Rhodes and Keefer. The viscosity and the frozen thermal conductivity are in good agreement with the literature
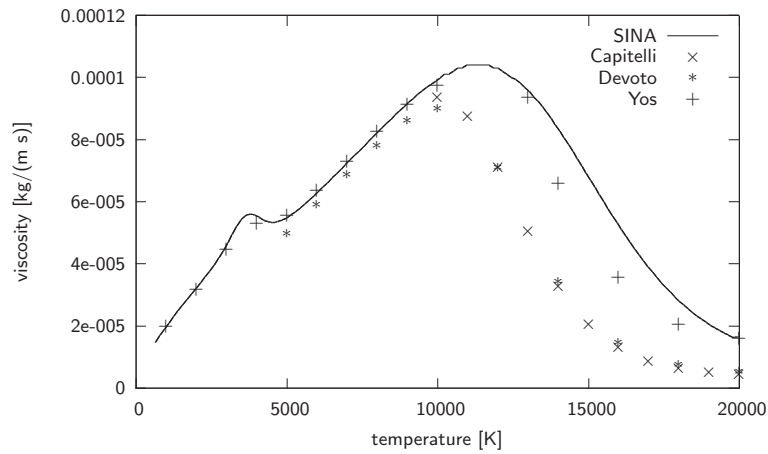
Figure 6. Viscosity computed with the model of Yos, composition computed with the modified reaction scheme of Scott
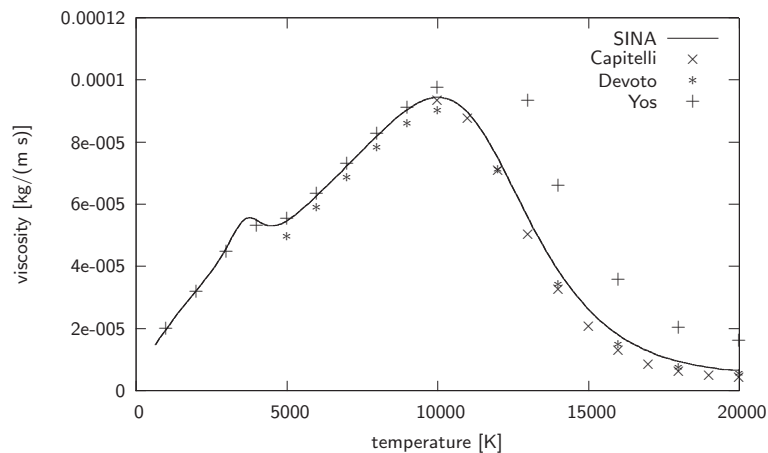

Figure 7. Viscosity computed with the model of CC, composition computed with the modified reaction scheme of Scott

only for temperatures below about 10000 K, as shown in Fig.s B and B for the viscosity and in Fig.s B and B for the frozen thermal conductivity. Above this temperature, the inaccurate chemical composition of the model of Rhodes and Keefer leads to a poor agreement of the transport coefficients. Thus, the chemistry model of Rhodes and Keefer is only advisable for plasma flows with high pressure and low temperature. Otherwise, the model of Scott should be used because of the accuracy of the chemical composition and of the transport coefficients, which of course depends significantly on the species concentration.

V. Conclusion

The hydrogen chemistry model of Rhodes and Keefer and the model of Scott are adopted for the use with SINA, as well as the model of Yos and the model of Chapman and Cowling for the computation of the according transport coefficients. For the model of Scott, the species H_3^+ and excited states had to be neglected due to a missing vibrational energy model and restrictions in SINA. The comparison of the chemistry models show that the model of Rhodes and Keefer does not predict the ionization of H correctly, while the modified model of Scott is in very good agreement with data from Patch[6] for both 100 Pa and 100000 Pa.

With both equilibrium compositions, the corresponding transport coefficients are computed with the model of Yos and the model of Chapman and Cowling. The model of Yos shows a good agreement with the
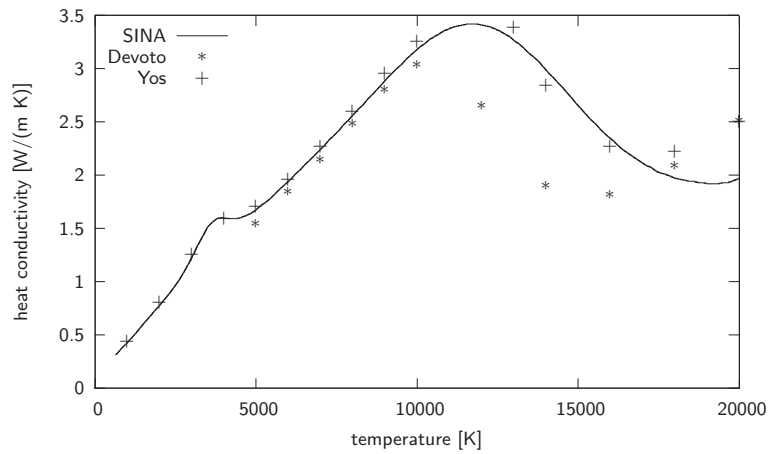
Figure 8. Frozen thermal conductivity computed with the model of Yos, composition computed with the modified reaction scheme of Scott
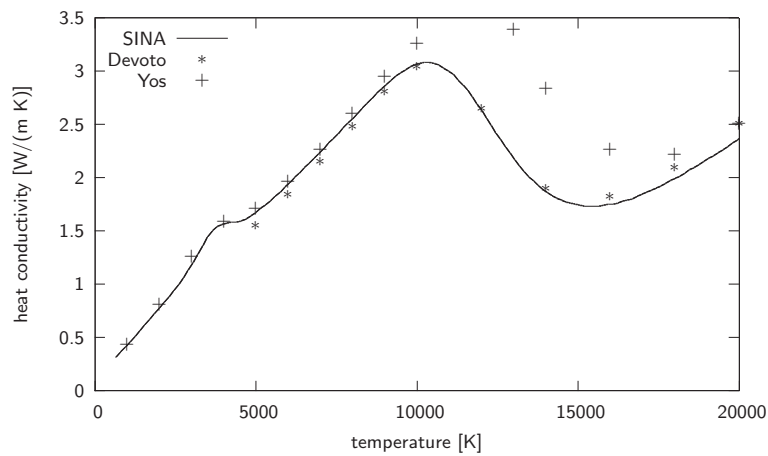

Figure 9. Frozen thermal conductivity computed with the model of CC, composition computed with the modified reaction scheme of Scott

data of Yos for the chemical composition of Scott. With the model of Rhodes and Keefer the agreement of the transport coefficients is not good because of the inaccurate representation of the ionization process in the chemistry model. The model of Chapman and Cowling shows a very good agreement with the data from Capitelli and Devoto. Again, the accuracy of the transport coefficients is degraded when using the poor chemistry model of Rhodes and Keefer.

In summary, the combination of the modified chemistry model of Scott and the Chapman and Cowling model for the transport coefficients can be recommended for the computation of hydrogen plasma flows. If the computational power is limited, the pressure is high and the temperatures are low, one can use the combination of Rhodes and Keefer for the chemistry and Chapman and Cowling for the transport coefficients without being too inaccurate. The model of Chapman and Cowling needs additional collision integrals for the higher approximation of the electron thermal conductivity, that are not always available or easy to determine. Then, the model of Yos is a good alternative.

The neglection of the ion H_3^+ is justified by the fact that its concentration is very low in equilibrium. It may influence the concentrations of other species, though, and may play a more important role in non-equilibrium. Both facts will be investigated in future, in combination with a consistent model for the vibrational energy of this three-atomic molecule. Also, the influence of the different models for chemistry and transport properties on the result of an thermal arcjet and a hybrid DC-RF thruster like TIHTUS ,[1]
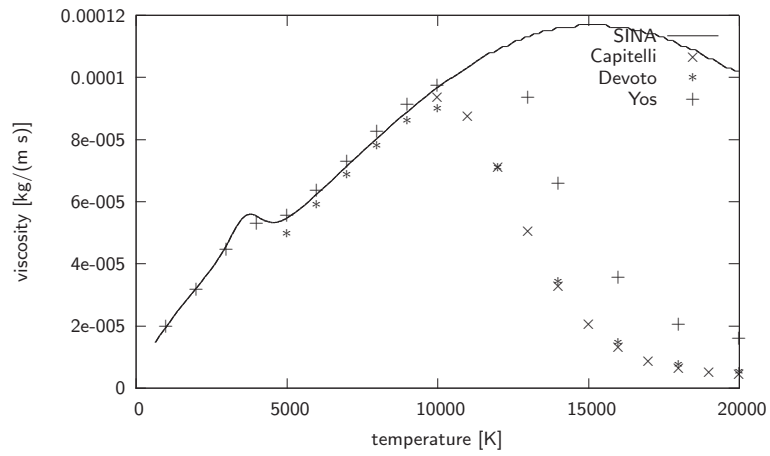
Figure 10. Viscosity computed with the model of Yos, composition computed with the reaction scheme of Rhodes & Keefer
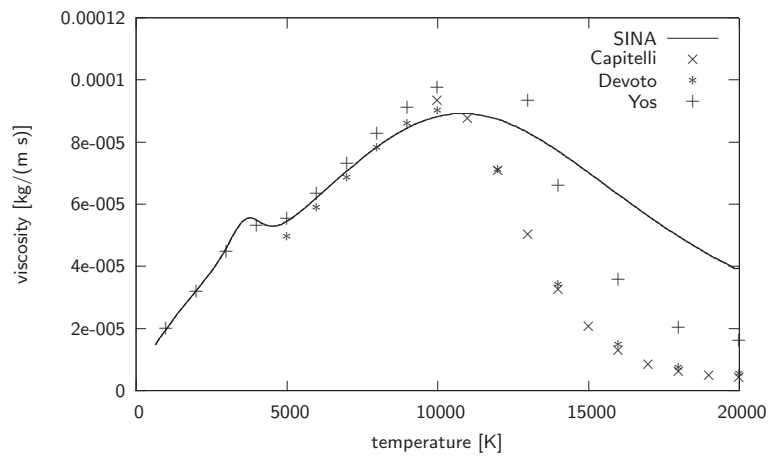

Figure 11. Viscosity computed with the model of CC, composition computed with the reaction scheme of Rhodes & Keefer

where the flow is in thermal and chemical equilibrium, will be investigated.
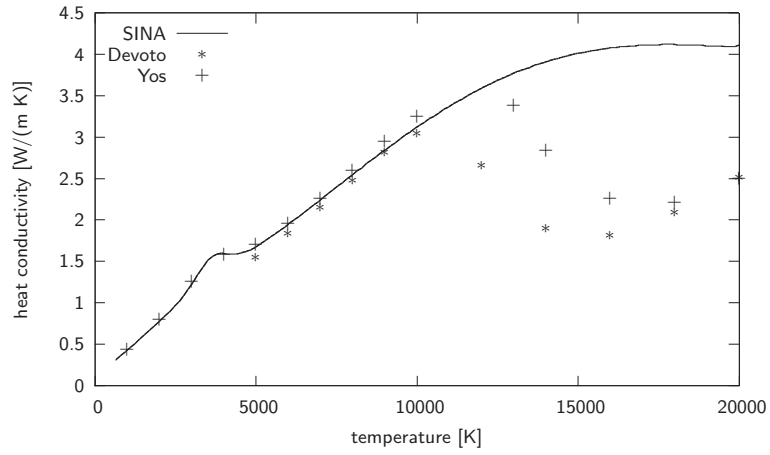
Acknowledgments

Figure 12. Frozen thermal conductivity computed with the model of Yos, composition computed with the reaction scheme of Rhodes & Keefer
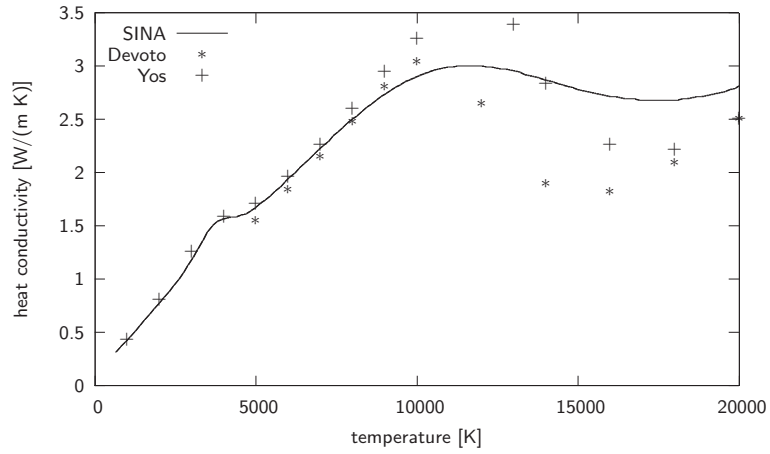

Figure 13. Frozen thermal conductivity computed with the model of CC, composition computed with the reaction scheme of Rhodes & Keefer

References

[1]Böhrk, H., *Zur induktiven Nachheizung einer Überschallwasserstoffströmung*, Ph.D. thesis, Institut für Raumfahrtsysteme, Universität Stuttgart, 2009.

[2]Bauder, U., Löhle, S., Petkow, D., Herdrich, G., Fasoulas, S., Fertig, M., and Auweter-Kurtz, M., "Current Numerical and Experimental Investigations of the Hybrid DC-RF Thruster TIHTUS," 2010.

[3]Bauder, U., Majid, A., Fertig, M., and Auweter-Kurtz, M., "Improvement and Extension of the Loosely Coupled Navier-Stokes Code SINA to Different Gases," 2010.

[4]Park, C., "On Convergence of Computation of Chemical Reacting Flows," AIAA-Paper 85-0247, 1985.

[5]Scott, C. D., "Determining Electron Temperature and Density in a Hydrogen Microwave Plasma," *Journal of Thermophysics and Heat Transfer*, Vol. 10, 1996.

[6]Patch, R. W., "Thermodynamic properties and theoretical rocket peformance of hydrogen to 100000 K and 1.01324×10^8 N/m^2," .

[7]Gurvich, L. V., Veyts, I. V., and Alcock, C. B., *Thermodynamic Properties of Individual Substances, Vol. 2*, Taylor & Francis, 1990.

[8]National Institute of Standards and Technology, *National Institute of Standards and Technology*.

[9]Rhodes, R. and Keefer, D., "Non-equilibrium modeling of hydrogen arcjet thrusters," .

[10]McCay, T. D. and Dexter, C. E., "Chemical Kinetic Performance Loss for a Hydrogen Laser Thermal Thruster," *J. Spacecraft*, Vol. 24, No. 4, 1987.

[11]Keefer, D., "The Theory and the Diagnosis of the Electrodeless Discharge," .

[12]Bates, D. R. and Snyder, R., "Application of Classical Finite Characteristic Collision Time Approximation to Ionization of Atomic Hydrogen by Electron Impact," *Journal of Physics, Part B - Atomic and Molecular Physics*, Vol. 8, No. 4, 1975.

[13]Fertig, M., Dohr, A., and Frhauf, H.-H., "Transport Coefficients for High-Temperature Nonequilibrium Air Flows," *Journal of Thermodynamics and Heat Transfer*, 1998.

[14]Fertig, M. and Herdrich, G., "The Advanced URANUS Navier-Stokes Code for the Simulation of Nonequilibrium Re-entry Flows," *Transactions of the Japan Society for Aeronautical and Space Sciences, Space Technology Japan*, Vol. 7, No. ISTS26, 2009, pp. Pe_15 − Pe_24.

[15]Gupta, R. N., Yos, J. M., Thompson, R. A., and Lee, K.-P., "A review of reaction rates and thermodynamic and transport properties for an 11-species air model for chemical and thermal nonequilibrium calculations to 30000 K," .

[16]Brandel, F., "Berechnung der Reaktionsraten und Transportkoeffizienten von Helium und Wasserstoff fr die Simulation eines thermischen Lichtbogentriebwerks," .

[17]Sleziona, P., "Hochenthalpiestrmungen fr Raumfahrtanwendungen," .

[18]Hirschfelder, J. O., Curtiss, C. F., and Bird, R. B., *The Molecular Theory of Gases and Liquids*, Wiley Interscience Publication, New York, 1966.

[19]Mason, E., Munn, R., and Smith, F., "Transport Coefficients of Ionized Gases," *Physics of Fluids*, 1967.

[20]Yos, J., "Transport Properties of Nitrogen, Hydrogen, Oxygen and Air to 30000K," .

[21]Lee, J., "Basic Governing Equations for the Flight Regimes of Aeroassisted Orbital transfer Vehicles," Vol. 96.

[22]Brokaw, R., "Approximate Formula for the Viscosity and Thermal Conductivity of Gas Mixtures," .

[23]Devoto, R., "Simplified Expressions for the Transport Properties of Ionized Monoatomic Gases," *Physics of Fluids*, 1967.

[24]Gorse, C. and Capitelli, M., "Collision integrals of high temperature hydrogen species," *Atomic and plasma-material interaction data for fusion*, Vol. 9, International Atomic Energy Agency, 2001.

[25]Laricchiuta, A., Colonna, G., Bruno, D., Celiberto, R., Gorse, C., Pirani, F., and Capitelli, M., "Classical transport collision integrals for an Lennard-Jones like phenomenological model potential," *Chemical Physics Letters*, , No. 445, 2007.

[26]Höptner, J., *Numerische Simulation der chemischen Reaktionen und der Transportkoeffizienten von Wasserstoff*, Universität Stuttgart, 2010.

[27]Hermann, J. A., "Modellierung der Wasserstoff-Nichtgleichgewichtschemie und Implementierung des Modells in ein Programm zur Berechnung eines stationr brennenden elektrischen Lichtbogens," .

[28]Capitelli, M., Celiberto, R., Gorse, C., Laricchiuta, A., Pagano, D., and Traversa, P., "Transport properties of local thermodynamic equilibrium hydrogen plasmas including electronically excited states," *Physical Review*, , No. 69, 2004.

[29]Devoto, R. S., "Transport coefficients of partially ionized hydrogen," *Journal of Plasma Physics*, Vol. 2, 1968.